RESEARCH PAPER

Enhancing anticancer efficacy via nutraceutical co-delivery of resveratrol and borage oil using nanostructured lipid carriers in non-small cell lung cancer

Swati K. Kurtkoti[1*], Harshaben V. Patel[1], Ashok N. Mahajan[1]

[1]Department of Pharmaceutics, Indukaka Ipcowala College of Pharmacy, The Charutar Vidya Mandal (CVM) University, New Vallabh Vidyanagar, Anand, Gujarat-388121, India

[*]Corresponding Author: Swati K. Kurtkoti, Email: swati.kurtkoti@cvmu.edu.in, Mobile: 7573092430

ABSTRACT

Background: Resveratrol, a nutraceutical, is broadly examined for its anticancer properties against non-small cell lung cancer (NSCLC). However, its clinical translation is halted due to its poor water solubility, quick metabolism, poor oral bioavailability, and dose dependent activity. Borage oil, a nutraceutical lipid rich in γ-linolenic acid (GLA), is a lipophilic nutraceutical with inherent anticancer properties; however, its applicability in cancer therapy is inadequately explored. The current study investigates the development of a rational nanotechnology-based strategy to enhance anticancer efficacy of resveratrol using a bioactive excipient in NSCLC.

Methods: Nanostructured lipid carriers (NLCs) were developed using melt-emulsification-ultrasonication technique to co-deliver resveratrol and borage oil. A 3^2 full factorial design was used to optimize the formulation parameters. The optimized NLCs were characterized for particle size, polydispersity index, zeta potential, encapsulation efficiency, and in vitro release kinetics. The synergism between borage oil and resveratrol and the combined antiproliferative effects were studied using MTT assay in A549 cell lines.

Results: The resveratrol to borage oil in a ratio of 1:5 (Q = 1.25) showed an optimum synergy for anticancer effect. The optimized NLCs showed the particle size ~100 nm with a narrow size distribution. The encapsulation efficiency was found to be 98.53%, with good stability. The in vitro drug release showed a sustained effect. Compared to free drug and non-bioactive lipid-based NLCs, the co-delivery system of the nutraceutical showed significantly improved antiproliferative efficacy, a 3.8-fold and 1.45-fold reduction in IC50 compared to free resveratrol and conventional lipid carriers respectively.

Discussion: The enhanced anticancer activity of the co-delivery system can be attributed to the synergistic effect of resveratrol and GLA rich borage oil, the bioactive excipient instead of a passive carrier. The optimized NLC formulation showed improved drug solubilization, retention, and sustained release, ultimately leading to enhanced biological activity.

Conclusion: The findings establish the potential of a bioactive excipient in nanostructured lipid carriers as a nutraceutical co-delivery system for cancer therapy. Using bioactive dietary lipids such as GLA-rich borage oil, the function of excipient beyond their role as passive carriers can be explored. This nutraceutical bioactive excipient driven approach offers a promising platform for improving anticancer efficacy in NSCLC using advanced drug delivery systems.

Keywords: Nutraceuticals, Nanostructured lipid carriers, resveratrol, borage oil, synergistic drug delivery, Non-small Cell Lung Cancer.

How to cite this article: Kurtkoti SK, Patel HV, Mahajan AN. Enhancing anticancer efficacy via nutraceutical co-delivery of resveratrol and borage oil using nanostructured lipid carriers in non-small cell lung cancer. Int J Drug Deliv Technol. 2026;16(51s): 590-609. DOI: 10.25258/ijddt.16.51s.44

Source of support: Nil.

Conflict of interest: None

Introduction

Cancer, cardiovascular disorders, metabolic syndromes and neurodegenerative diseases formas a part of chronic diseases with the most burdensome health problems globally. Despite the tremendous research being conducted across the globe development of a long-term, safe, targeted therapeutic strategies to manage these pathologies is still far to achieve. Nutraceuticals is a growing area that explores the potential of food based therapy due to its pleiotropic effects and good safety profile. Using nutraceuticals either as a standalone drug or incorporating it as bioactive compound for adjuvant therapy, opens a wide scope for establishing successful strategies for long term management of chronic disease.

Nutraceuticals is an age-old traditional practice of using food as medicines. With the onset of biotechnology and nanotechnology, nutraceuticals have recently been in spotlight not only for preventing nutritional deficiency but also for managing a chronic disease. Nutraceuticals have showed to target multiple molecular pathways that are involved in the development and progression of a disease. Studies on naturally derived polyphenols, fatty acids, and secondary plant metabolites have found proven antioxidant, anti-inflammatory, immunomodulatory, and cytoprotective activities. These results can be leveraged in treatment of chronic diseases such as cancer with complex multifactorial pathophysiology. Further, the safety profile and no long-term adverse effects, makes the nutraceuticals promising candidates for supportive and preventive therapies. Despite the plethora of beneficial effects of nutraceuticals, due to their inherent properties such as poor water solubility and variable pharmacokinetics, the clinical translation is hampered.

One of the major chronic disease burdening and challenging the healthcare system worldwide is lung cancer. Lung cancer is to date the linked to disease with highest mortality rate among both men and women [1–3]. Studies on epidemiological records have been indicative of the fact that around 80–85% of lung cancer can be categorized to non-small cell lung cancer (NSCLC) type. NSCLC is a subtype of lung cancer that is distinguished based on its violent tumour growth and rapid progression of cancer [4,5]. The overlapping symptoms of NSCLC to COPD and asthma often hinders the early-stage diagnosis of this disease. Further, development of both innate and acquire drug resistance and severe adverse effect of conventional chemotherapy and radiation therapy, often leads to poor prognosis. This has led to a pressing and continuous need for alternative or complementary therapeutic approaches that offer multi-targeted efficacy with reduced systemic toxicity such as those seen with nutraceuticals in cancer models [6].

The emergence of nanotechnology and development of nanobiotechnology based drug delivery systems shifted the approaches in the cancer therapeutics. Nanotechnology based carrier systems have not only improved the bioavailability and stability of drug but also helped achieve targeted delivery of therapeutic agents [7-10]. These nanoscale systems have shown to improve pharmacokinetic profiles while minimizing systemic adverse effects via controlled and targeted mechanisms. These platform technologies are more valuable for nutraceuticals and bioactive compounds that suffer from poor solubility, instability, and unfavourable pharmacokinetic profiles.

Among the various nanocarrier systems, nanostructured lipid carriers are considered an advanced colloidal platform. NLCs consist of a binary mixture of structurally different components, namely solid and liquid lipids. [11,12]. The unique formulation-based architecture of NLCs, generates a flexible, less orderly lipid matrix that can improve the bioavailability, physicochemical stability, and controlled release properties of poorly soluble compounds [13-15].

Resveratrol (RSV) is a naturally occurring polyphenolic nutraceutical. Chemically it is a stilbene (3,5,4′-trihydroxy-trans-stilbene) widely available from grapes, cherries and watermelon. RSV has been under investigation for its versatile anticancer properties. Acting via the three major pathways i.e., inhibition of cancer cell proliferation, induction of apoptosis, and suppression of angiogenesis, RSV has proved to be an excellent candidate for anticancer drug especially in breast cancer [16-18]. RSV acts via modulation of critical cellular pathways [19], such as cell cycle arrest, mitochondrial-mediated apoptosis, and regulation of inflammatory responses [20]. However, several pharmacological limitations of RSV, such as poor aqueous solubility, low systemic bioavailability, and dose-dependent biphasic pharmacological effects have hindered the clinical translation of RSV [21-23]. One of the unique characteristics of RSV is it's does dependent response. RSV in low doses (30-150mg daily) has been used as a nutraceutical especially for its cardiovascular and antiaging properties [24]; however, a striking contradiction is the paradoxically function of RSV at higher doses. At higher doses, the drug acts as a pro-oxidant and induces cellular toxicity. Furthermore, rapid metabolic degradation, including extensive first pass and pulmonary metabolism [25], and short elimination half-life further compromise its therapeutic potential in lung cancer therapy. The restrictions underscore the necessity of formulation-based pharmacokinetic optimization to facilitate successful clinical translation. The solution of these problems allows NLCs to significantly improve therapeutic efficacy and reduce dose-related adverse effects, which opens new possibilities in clinical use, particularly in the targeted delivery approach, including the pulmonary administration of lung cancer treatment [26-29].

A rational formulation strategy does not only work to enhance the efficiency of the delivery. A rational formulation strategy has changed the focus to the exploitation of the inherent bioactivity of excipients to improve therapeutic responses. The pharmaceutical principle of unification of medicines and excipients evolved out of the traditional principle of *materia medica* focuses on the synergistic interaction of active pharmaceutical substances and excipients. This concept has by far advocated the selection of excipients from mere formulation aspects to greater enhanced therapeutic efficacy [30]. This approach can be very well incorporated in nutraceutical formulation, where excipients can be selected to contribute intrinsic bioactivity alongside the drug. Using this approach the excipients are deliberately chosen to complement and optimize the pharmacological properties of the primary therapeutic agent, thereby improving overall efficacy, including the anticancer effect while reducing adverse effects [31]. Studies conducted by researchers [32] have established that gamma-linolenic acid (GLA) rich polyunsaturated fatty acids, exhibit significant apoptotic activity, particularly improved efficacy in breast and lung cancer cell line models [33,34]. Several fixed oils have been found to contain subsequently high concentration of GLA. Some noteworthy GLA rich oils include borage oil (18-26g GLA/100g),

blackcurrant seed oil (15-20g GLA/100g), evening primrose oil (7-10g GLA/100g) and fungal (23–26 g GLA/100g) [35]. Using a nutraceutical oil that is rich in GLA, as an excipient, the unification strategy can be used to substantially enhance the overall therapeutic potential, particularly in the treatment of NSCLC. By incorporating resveratrol and GLA-rich oil within nanostructured lipid carriers for pulmonary delivery, this approach leverages the synergistic bioactive effects of both components, resulting in improved drug loading capacity, enhanced system stability, superior bioavailability, and site-specific delivery to lung cancer cells.

Therefore, the present study aims to synthesize and characterize nutraceutical-enabled lipid-based hybrid nanostructured carriers incorporating a γ-linolenic acid–rich bioactive excipient with the aim of enhancing the anticancer efficacy of resveratrol against non-small cell lung cancer. [

Methods and Materials

Materials

Resveratrol (RSV) was purchased from Yucca Enterprises, Mumbai, India. The lipid excipients oleic acid (OA) and borage oil (18–26% GLA concentration) were acquired from Sisco Research Laboratories Pvt. Ltd., India, and Deve Herbes, India, respectively. Soy lecithin and Tween 80 were purchased from S D Fine Chem Ltd. in Mumbai, India. Merck (Darmstadt, Germany) supplied methanol, chloroform, and other analytical-grade solvents. The National Centre for Cell Sciences (NCCS) in Pune, India, provided the Human Lung Adenocarcinoma cell line (A549), which was cultivated in accordance with accepted institutional procedures.

Screening of Solid Lipids

Different solid lipids were evaluated systematically for selecting the optimum lipid matrix to incorporate RSV. Commonly available solid lipids such as glyceryl behenate (Compritol 888ATO), stearic acid, tristearin, carnauba wax, beeswax, and glyceryl monostearate were chosen. The accurate weight of 500 mg solid lipid was transferred into 3 mL glass vials. Each lipid was heated at a temperature of 5°C above the melting point of each lipid to obtain the molten lipid. To the molten lipid, RSV was then added incrementally in small portions under continuous gentle stirring. After each addition, the mixture was allowed to equilibrate for 10 minutes at the maintained temperature and observed visually under ambient light for complete solubilization. The addition of RSV was continued until no further dissolution was observed. The total amount of RSV solubilized per gram of lipid was recorded as the solubility value. The experiment was performed in triplicate (n = 3) and results are expressed as mean ± standard deviation [36,37].

Liquid Lipids Screening

GLA rich liquid lipids, viz. Borage oil, evening Primrose oil and blackcurrant seed oil were also tested on the solubility of RSV [35,38,39]. One ml of each oil was put in a 2 mL amber glass vial with a seal, and an overload of (~50 mg) RSV was added. The vials were vortexed briefly (30 s) to obtain initial dispersion, and the mixtures were then put on an orbital mixer incubator at 100 rpm and 25°C to allow saturation of equilibrium solubility. Next, the samples were centrifuged at 5000 rpm for 15 minutes at 25°C to settle the undissolved drug. The supernatant was aspirated and diluted with appropriate volume of methanol then spectrophotometrically measured at 306 nm with a UV-Visible spectrometer. The experiment was repeated thrice (n = 3), and the results are presented as the mean and standard deviation [36].

Surfactant Screening

The ability of the surfactant to emulsify the lipid mixture is a key parameter which defines the size of the particle and polydispersity index (PDI) of nanoparticulate systems. The surfactants and combinations of surfactants were also tried to find the best emulsification system. Preliminary NLC formulations (30 mL) were made by the addition of 1% w/v lipid mixture (Solid lipid: Liquid lipid = 2:1), 3% w/v surfactant or surfactant mixtures as indicated in Table 1. Initial NLCs were prepared through melt homogenization and then probe sonication using a Branson Digital Sonifier (Branson Ultrasonics, USA) at 85% amplitude with 30 seconds on and 10 seconds off pulse intervals resulting in a total processing time of 5 minutes. Sonication was done in an ice bath to avoid the thermal degradation of lipid emulsion. Particle size and PDI were measured using dynamic light scattering (DLS) technique with a NanoPartica SZ-100 instrument (Horiba, Japan). Physical stability of pre-NLCs was monitored for phase separation, precipitation, or changes in optical transparency following one week of storage at room temperature prior to final surfactant selection [40].

Table 1 Preliminary NLC batch for screening of surfactant

Batch	Lipid Used (1%w/v)	Surfactant Used	Particle Size	PDI
S1	Tristearin + Borage Oil	Tween 80	98.40 nm	0.45
S2	Tristearin + Borage Oil	Poloxamer 188	124.67 nm	0.70
S3	Tristearin + Borage Oil	Tween 80 + Span 80 (1:1)	87.56 nm	0.28
S4	Tristearin + Borage Oil	Poloxamer 188 + Span 80 (1:1)	100.60 nm	0.48
S5	Tristearin + Borage Oil	Tween 80 + Soy lecithin (1:1)	54.23 nm	0.18

In Vitro Synergistic Studies of Borage Oil Combined with Resveratrol

The optimum concentration of liquid lipid component was determined based on effect of liquid lipid on the cancer cells. To determine the synergistic ratio between RSV and borage oil, extensive in vitro synergistic studies were conducted. The cellular viability was assessed using the MTT (3-(4,5-dimethylthiazol-2-yl)-2,5-diphenyltetrazolium bromide) test. The Human Adenocarcinoma Cell Lines (A549 cells) were cultivated at 37°C in a humidified environment with 5% CO2 in Ham's F12 medium supplemented with 10% fetal bovine serum (FBS) and 2.5% antibiotic cocktail. To improve cellular adhesion, A549 cells (5×10^3 cells per well) were put to 96-well plates and incubated for a full day.

After the initial incubation period, 100 µL of test formulations were substituted for the entire culture medium. These formulations included: (i) RSV dissolved in isopropanol (0.1 g/L); (ii) borage oil solutions prepared in isopropanol at different concentrations (0.1, 0.2, 0.5, 0.8, 1.0, and 1.5 g/L); and (iii) combination formulations of RSV and borage oil at different ratios (1:1, 1:2, 1:5, 1:8, and 1:10) to establish synergistic relationships. Following this incubation, 50µL of dimethyl sulfoxide (DMSO) was added to each well to dissolve the formazan crystals following the removal of 85µL of media. A microplate reader was used to record absorbance readings at 570 nm.

The following formula was used to determine the combination index (Q-value) and the percentage of cell proliferation inhibition:

$$Q = \frac{E_{ab}}{E_a + E_b - E_a E_b}$$

where E_{ab} represents the inhibition rate of the combination formulation, and E_a and E_b represent the inhibition rates of individual components, respectively [41,42].

Preparation of Nanostructured Lipid Carriers

Nanostructured lipid carriers containing the bioactive excipient borage oil (BONLCs) were formulated using melt-emulsification -sonication technique. Borage oil and tristearin were heated at 70°C to get a molten mass. Throughout all formulations, the drug to liquid lipid ratio (RSV: borage oil) was maintained constant at 1:5 (w/w) based on the optimum synergistic ratio established from in vitro cytotoxicity studies. The total lipid content was maintained at 1% w/v relative to the aqueous phase in all formulations. RSV was dissolved in this molten binary mixture of borage oil and tristearin to ensure homogenous drug distribution. Aqueous phase was prepared by dissolving Tween 80 and soy lecithin (1:1 w/w) at surfactant concentrations according to the experimental design (1.5% -4.5% w/v) in double-distilled water and heated to 70°C before emulsification. The lipid phase was emulsified with an aqueous phase while being continuously stirred for 5 mins at 1000 rpm using a magnetic stirrer at 70°C. To create a coarse emulsion, high-shear homogenization was carried out for ten minutes at 10,000 rpm using an IKA T25 Ultra-Turrax homogenizer (IKA, Germany). A Branson Digital Sonifier (Branson Ultrasonics, USA) was used to subject the emulsion to probe sonication (5 minutes, 85% amplitude, 30-second pulse intervals) to further reduce droplet size and create nanostructures. The resulting hot nano emulsion was rapidly cooled in an ice bath over 20 minutes to promote the crystallization of lipids and the formation of NLC. NLC dispersion (30 mL) was obtained in each batch, and the formulations were prepared in triplicate (n = 3) on different days to ensure that the batch-to-batch reproduction is maintained [43].

Similarly, NLC were also fabricated using a conventional liquid lipid (oleic acid) [15,27,29]. The oleic acid-based nanostructured lipid carriers (OANLCs) were prepared using the same experimental conditions utilized for fabricating BONLCs.

Experimental Design and Optimization

For the optimization of the formulation, the single-factor investigation (OFAT) was carried out to initially screen the variables. The binary lipid mixture concentration (1% w/v), homogenization time (5 minutes), homogenization speed (10,000 rpm), and sonication amplitude (85%) were all kept constant throughout the optimization study based on preliminary results, guaranteeing a medication to liquid lipid ratio of 1:5. After initial screening trials, critical formulation parameters were carefully varied thanks to a 3^2 complete factorial design.

The independent variables chosen for optimization under a 3^2 factorial design was the drug-to-total lipid ratio (X_1). Since the drug to liquid lipid ratio was fixed at 1:5 (w/w) throughout the study, varying the drug to total lipid ratio (X_1) across three levels (1:10, 1:15, and 1:20) resulted in a proportional variation in the solid lipid (tristearin) content. This consequently yielded solid: liquid lipid ratios of 1:1, 2:1, and 3:1 at drug: total lipid ratios of 1:10, 1:15, and 1:20 respectively, as summarized in Table 2. The second independent variable chosen was the surfactant concentration

(X_2). The surfactant concentration (X_2) was varied across three levels (1.5%, 3.0%, and 4.5% w/v), comprising a 1:1 binary mixture of Tween 80 and soy lecithin throughout all formulations. The specific surfactant concentration used in each of the nine experimental formulations is detailed in **Table 2.**

The dependent variables (responses) that were evaluated were particle size (Y_1), polydispersity index (Y_2) and encapsulation efficiency (Y_3). Nine experimental formulations (F1–F9) were generated using Design-Expert statistical software (Stat-Ease Inc., USA) according to the factorial design matrix. Independent variables were coded at three levels (-1, 0, +1) corresponding to low, medium, and high values, respectively [44]. During the studies the drug to liquid lipid ratio was maintained constant (1:5).

The experimental design matrix with coded and actual values is presented in **Table 2**. The 3^2 factorial design allows for systematic evaluation of main effects and interaction effects between the two factors. Both linear and quadratic polynomial models were fitted to the experimental data, and statistical analysis was used to identify important model terms ($p < 0.05$). The adequacy of the developed model was evaluated using coefficient of determination (R^2), modified R^2, expected R^2, and suitable precision values. Analysis of variance (ANOVA) was used to determine the significance of each factor and their interactions. Lack-of-fit tests were used to evaluate model validity ($p > 0.05$ indicates non-significant lack-of-fit), confirming the predictive power of the established models [45].

Table 2: 3^2 Factorial Design Matrix and Response Variables for NLC Formulations

Formulation	X_1	X_2	Y_1: Particle Size (nm)	Y_2: PDI	Y_3: EE (%)
F1	-1	-1	158.3 ± 6.2	0.42 ± 0.04	89.45 ± 2.31
F2	-1	0	121.5 ± 4.8	0.31 ± 0.03	93.78 ± 1.87
F3	-1	+1	95.7 ± 3.9	0.24 ± 0.02	94.32 ± 1.54
F4	0	-1	182.4 ± 7.5	0.48 ± 0.05	91.23 ± 2.12
F5	0	0	132.8 ± 5.2	0.29 ± 0.03	95.67 ± 1.43
F6	0	+1	98.2 ± 4.1	0.26 ± 0.02	96.15 ± 1.28
F7	+1	-1	215.6 ± 8.9	0.54 ± 0.06	88.76 ± 2.45
F8	+1	0	168.9 ± 6.7	0.38 ± 0.04	93.45 ± 1.76
F9	+1	+1	125.3 ±	0.31 ±	94.89 ± 1.52

	5.4	0.03		
Independent Variable	**Coded Symbol**	**Low Level (-1)**	**Medium Level (0)**	**High Level (+1)**
Drug: Total lipid Ratio	X_1	1:10	1:15	1:20
Surfactant Concentration (% w/v)	X_2	1.5	3.0	4.5

Data presented as mean ± standard deviation (n = 3)

Physicochemical Characterization of NLCs

A thorough physicochemical characterization of the optimized batch of NLCs was done. After proper dilution, the formulation was analyzed in terms of particle size distribution, polydispersity index (PDI) and zeta potential, using dynamic light scattering technique with the assistance of High efficiency particle size analyzer and zeta potential measuring system, NanoPartica SZ-100 analyzer (Horiba, Japan).

Surface morphology was studied using transmission electron microscopy (TEM). Samples were prepared by placing a drop of diluted NLC dispersion on a carbon-coated copper grid, negatively stained with 2% phosphotungstic acid, and examined using FEG - Transmission Electron Microscope (HR-TEM), Talos F200i S/TEM (HRTEM-200KV), (Thermo Fisher Scientific), operated at appropriate accelerating voltage.

For determination of percentage encapsulation efficiency (EE (%)) the NLC dispersions were centrifuged using a refrigerated centrifuge **(10,000 rpm at 4°C for 30 min)** to separate free drug from encapsulated drug. The supernatant containing free drug was carefully aspirated and analyzed spectrophotometrically at 306 nm, after proper dilution. Encapsulation efficiency (EE%) was calculated using the following equations:

$$EE(\%) = \frac{Total\ Drug - Free\ Drug}{Total\ Drug} \times 100$$

In Vitro Drug Release Studies

The in vitro drug release kinetics of RSV from different NLC formulations were evaluated using the standard dialysis bag diffusion method. The dialysis bags with a molecular weight cut-off of 12,000-14,000 Da, were pre-soaked in release medium for 24 hours before conducting the experiment. 2mL of NLC dispersions were accurately placed in a dialysis bag and were sealed. Artificial lysosomal fluid (ALF, pH 4.5), was chosen as the release medium. To achieve physiological relevance to the applications of pulmonary delivery, the acidic pH of the release medium was selected to mimic the lysosomal environment of lung macrophages [46-48]. The dialysis bags were placed in 50 mL of release medium and allowed to incubate at 37°C with constant stirring of 100rpm. The samples (1mL) were withdrawn aa predetermined time intervals (0.5, 1, 2, 4, 6, 8, 12, 24, 36, and 48 hours). The mediums of release were substituted with equal portions of fresh ALF to keep sink conditions constant. The amount of released RSV was determined using UV-visible spectrophotometry at 306 nm. To study the release kinetics, cumulative drug release profiles were built. The mathematical models (zero-order, first-order, Higuchi, and Korsmeyer-Peppas) were used to analyze the data and explain the drug release mechanisms [49-52].

Cytotoxicity Assessment Using MTT Assay

The antiproliferative effect and

cytotoxicity of free RSV, BONLCs, and OANLCs were detected using the MTT colorimetric assay. The Human Adenocarcinoma Cell lines (A549) were utilized for the MTT assay. The culturing of cells was done in 96-well plates maintaining the density of cells in each well around 5×10^3 cells. Post culturing the plates were incubated for 24 hours. This facilitated cell adhesion to the wells. Each well was subsequently treated to different concentrations of test formulations (ranging from 1 to 100 µM RSV) and incubated for 48 hours. After 48hours of treatment, the culture medium was removed from the wells by aspiration. This was followed by incubation with 0.5mg/mL of MTT reagent for additional 4 hours maintaining the temperature 37°C, to allow formation of formazan crystals. The crystals were then solubilized using DMSO and the absorbance was recorded using SpectraMax M2e & Multidetection microplate reader (Molecular Devices, USA) at 570nm. Cell viability was calculated as percentage relative to untreated control cells. The IC_{50} values were determined using non-linear regression analysis. The cytotoxicity profiles were compared to determine the increase in resveratrol potency with the aid of NLC-mediated delivery, with the bioactive role of borage oil as a functional lipid carrier being a special focus [32].

Discussion and results

Solid Lipid Screening

The choice of a solid lipid is one of the important steps in establishing the performance of NLC. Not only does it affect the drug solubility, but it also affects the encapsulation efficiency, and release kinetics [36]. In the current study, several solid lipids such as compritol 888ATO, stearic acid, tristearin, carnauba wax, beeswax and glycerol monostearate were evaluated in a systematic manner on their capacity to solubilize resveratrol. **Fig. 1a** illustrates the solubility of RSV in various solid lipids with all the lipids screened, tristearin exhibited the greatest resveratrol solubility (0.8 mg/g) and was therefore chosen as the solid lipid matrix to be used in subsequent NLC fabrication. It is possible to assume that the high solubilization ability of tristearin is explained by its molecular structure and crystal polymorphism, which form unfavorable hydrophilic interactions with the lipophilic resveratrol molecule. Moreover, tristearin has the right melting properties and creates a stable lipid matrix that assists in the controlled release of drugs [45].

Liquid Lipid Screening

In nutraceutical delivery systems, where long-term safety and metabolic compatibility are crucial for applications involving chronic diseases, the choice of biocompatible lipid excipients is especially crucial. GLA-rich plant oils are popular choices for bioactive excipient selection since they are well-known nutraceuticals with proven anti-inflammatory and anticancer qualities. Finding an appropriate lipid phase for NLC formulation was the goal of the solubility screening of RSV in GLA-rich liquid lipids. The solubility screening of RSV in GLA-rich liquid lipids was conducted with the aim of finding a suitable lipid phase for NLC formulation. The solubility of RSV in different GLA-rich liquid lipids is shown in **Fig. 1b** Among the tested oils, namely borage oil, evening primrose oil, and blackcurrant seed oil, borage oil showed the highest solubilizing capacity toward RSV (3 mg/ml).

Borage oil exhibited better RSV solubility than all other options, due to a higher content of γ-linolenic acid (~20–25%) and unsaturated fatty acids, which generally enhance the solubilization of polyphenolic compounds by hydrophobic interactions. On the other hand, evening primrose oil and

blackcurrant seed oil, though containing GLA, had lower solubilizing capacities compared to borage oil, which is probably related to differences in the total lipid composition and to the presence of shorter or more saturated chains of fatty acids that reduce drug miscibility.

The enhanced solubilization in borage oil indicates favorable lipid-drug compatibility, which is essential for enhancing encapsulation efficiency, thereby ensuring stable incorporation of RSV within the lipid matrix of NLCs. Due to its enhanced solubility in RSV and possible enhancement of drug loading and release characteristics, borage oil, a nutraceutical oil with a high GLA content, was selected as a further formulation development as the liquid lipid component.

Surfactant Screening

Surfactants play an important role in influencing the particle size distribution and physical stability of NLC formulations [40]. Several surfactants and surfactant mixtures were systematically evaluated based on their required hydrophilic-lipophilic balance (RHLB) values relative to the composition of the lipid phase (**Table 1**). Binary combinations of the surfactants and single surfactants were examined like Tween 80, soy lecithin, poloxamer 188, and Span 80. The smallest particle size (54.23 nm) with an appropriate polydispersity index (0.18), indicating a narrow distribution of size, was obtained with a 1: 1 binary mixture of Tween 80 and soy lecithin, as seen in **Fig. 1c**. This surfactant mixture also demonstrated excellent physical stability in seven days at room temperature, demonstrating no observable phase separation, particle aggregation or optical clarity alterations. The synergistic stabilization mechanism is due to complementary molecular interactions: soy lecithin is a naturally occurring phospholipid mixture with hydrophobic acyl chains anchoring on the lipid particle surface and electrostatic stabilization by negatively charged phosphate groups, Tween 80 is a high HLB (15.0) non-ionic surfactant that stabilizes sterically at the oil-water interface [53,54].

This combination of surfactants has distinct advantages as far as pulmonary delivery is concerned. Both Soy lecithin and Tween 80 are of low pulmonary toxicity and are highly biocompatible [27]. There is inherent good biocompatibility of soy lecithin, which is an endogenous phospholipid component of lung surfactant, with pulmonary tissues and can aid better interaction with alveolar epithelial cells. Naturally derived surfactants like soy lecithin are also used as it is in line with the principles of nutraceutical formulation, which focus on biocompatibility, physiological relevance, and the ability to be administered on a repeated or chronic basis.

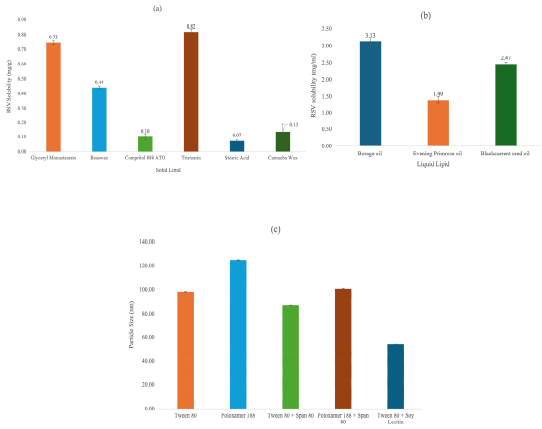

Fig. 1. Resveratrol solubility in various a) solid lipids b) GLA-rich liquid lipids; 1c particle size of preliminary NLCs

formulated using different surfactants and blends of surfactants.

In Vitro Synergistic Studies of Borage Oil Combined with RSV

An important element of NLC design is the proper choice of a nutraceutical liquid lipid component, particularly when it is applied to the medicine-excipient unification technique. The optimal combination of resveratrol and borage oil was established by conducting widespread in-vitro cytotoxicity studies on A549 NSCLC cells. All the molecules were moderately cytotoxic; RSV had an IC_{50} of approximately 40μM, whereas borage oil (because of its GLA content) had an IC_{50} between 200 and 300μM. Combination therapies on the other hand were proving to have synergistic advantages that were concentration dependent.

Microscopic observation of treated cells confirmed the synergistic interaction by visualizing significant morphological changes indicative of cellular disruption including cell shrinkage, membrane blebbing and nuclear condensation, which are characteristic of apoptotic cell death (**Fig. 2**).

Each ratio was calculated at known pharmacological standards [55-57] and interpreted as follows: $Q > 1.15$ is synergistic effects; $0.85 \leq Q \leq 1.15$ is additive effects; and $Q < 0.85$ is antagonistic effects. The calculated Q-values for RSV:Borage oil ratios of 1:1, 1:2, 1:5, 1:8, and 1:10 were 0.94, 1.16, 1.25, 0.86, and 0.85, respectively. The best synergistic ratio of RSV:Borage oil was 1:5 (Q = 1.25). RSV:Borage ratios 1: 1 and 1: 2, however, had only additive effects (Q = 0.94 and 1.16, respectively), but ratios 1: 8 and 1: 10 exhibited a tendency towards antagonism, which suggested that borage oil in excess concentration could inhibit resveratrol activity. These results led to the selection of 1:5 RSV borage oil ratio as the basis of NLC formulation research. These findings provide clear experimental evidence that in rationally optimized nutraceutical-nutraceutical combinations, synergistic anticancer effects can be generated rather than additive ones.

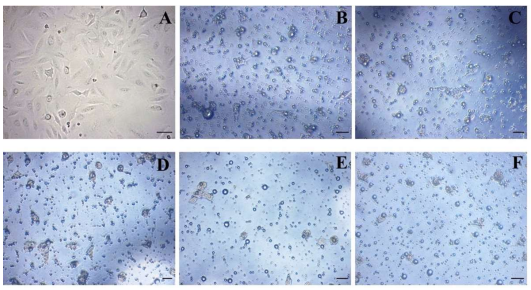

Fig. 2. The microscopic images of in vitro synergistic activity studies using A549 cells for A) control group B) 1:1 ratio of RSV to BO C) 1:2 ratio of RSV to BO D) 1:5 ratio of RSV to BO E) 1:8 ratio of RSV to BO and F) 1:10 ratio of RSV to BO.

Statistical Optimization Using 3^2 Factorial Design

The 3^2 full factorial design enabled systematic optimization of the relevant formulation parameters by a deliberate consideration of primary effects, interaction effects, and analysis of the response surface. The factorial design matrix was used to generate and characterize nine experimental formulations (**Table 2**). The mathematical relationships between independent variables (drug-to-lipid ratio and surfactant concentration) and dependent responses (particle size, PDI, and encapsulation efficiency) were identified with the help of the response surface approach. Polynomial (quadratic with interaction terms) models were fitted to the experimental data of every response variable. Statistical analysis of ANOVA showed that all responses were very significant ($p < 0.0001$), and the lack-of-fit was not significant ($p > 0.05$), which confirms the appropriateness of the models to be used in predictions. The coefficients

of determination (R^2) of 0.9834, 0.9712 and 0.9623 of the particle size, PDI and encapsulation efficiency respectively indicate that there was a high correlation between the observed and the expected values. The required precision values (signal-to-noise ratio) were above 15 and this proved that all models had enough model discrimination ability [44].

The drug to lipid ratio (X_1) made a significant influence on all the responses that were investigated. The review of the key effects revealed that the positive change in all the three response variables was observed with the increase in drug-to-lipid ratio of 1:10 to 1:20. Surfactant concentration (X_2) had an inverse effect on the particle size and PDI, but positive effect on the entrapment efficiency.

As the drug-to-lipid ratio was increased, the mean size of the particles increased gradually with a value of 125.2 nm (low level) to 169.9 nm (high level). This positive relationship can be explained by the volume of lipid matrix that is needed to house the higher drug concentration, and this leads to higher dimensions of the nanoparticle. The increased lipid core offers a higher capacity of accommodation of drug molecules but also results in the overall size growth of the particle [45].

Nonetheless, a strong negative correlation was exhibited among the concentration of the surfactant (X_2) on the particle size. When the surfactant concentration was increased (low level, 1.5% w/v) up to high level (4.5% w/v), the dramatic particle size decreased to 106.4 nm (averaged in all ratios of drugs to lipids). This mechanistic effect may be explained by the increased interfacial coverage and a decrease in interfacial tension that allows more efficient droplet disruption in high-shear homogenization and probe sonication. Increased levels of surfactants can offer enhanced protection of new interfaces formed which avoids coalescence of particles and instead forms smaller and more stable nanoparticles [40].

Moreover, when the drug to lipid ratio is raised, the homogeneity of dispersion is deteriorated. Drug-to lipid ratio(X_1) had a positive influence on polydispersity index (Y_2). The mean PDI rose as X1 went on the negative to the positive as it rose to about 0.32 to 0.41 with an increase in drug loading, which showed the larger the loading the larger was the size of the particle. It means that an increase in drug loading disrupts the ability to form uniform nuclei during the hot-melt homogenization and following sonication, leading to a wider particle size distribution and higher PDI.

Significant negative correlation was observed between the surfactant concentration with PDI. The PDI values decreased from 0.48 (1.5% surfactant) to 0.27 (4.5% surfactant). Increased concentrations of surfactants improve the effectiveness of droplet breakup in hot-melt homogenization and downstream sonication that results in more homogenous nanoparticles. The higher supply of the surfactant facilitates the rapid development of the thick interfacial layer surrounding the molten lipid droplets, thereby giving better stearic and electrostatic stabilization. This will avoid coalescence on cooling and solidification and produce finer particle size distributions.

The effect of drug to lipid ratio on the entrapment efficiency (Y_3) showed a complex non-linear relationship. The highest encapsulation efficiency (95-96) at medium drug-to- lipid ratios (1: 3.5). Low drug concentration (1:10) resulted in underutilization of the lipid matrix capacity and excessively high drug concentration (1:20) neared the saturation limits which may result in drug expulsion during the lipid crystallization process [14].

The concentration of the surfactant showed moderate positive influence, and encapsulation was slightly higher at higher concentrations of surfactant. This is due to better droplet disruption during hot-melt

homogenization and sonication producing smaller molten lipid droplets with higher surface area-to-volume ratios. The increased interfacial area facilitates an increased drug accommodation in the lipid phase, which increases entrapment efficiency during subsequent cooling and solidification.

The 3^2 factorial designs will allow testing of the interaction effects of drug-to-lipid ratio and surfactant concentration. Statistical analysis showed that there are significant synergistic interactions ($p < 0.05$) between the responses of particle size and PDI. In particular, the effect of particle size decrease with increased concentration of surfactants was larger with higher drug-to-lipid ratios, and therefore, enough surfactants are especially important when working with formulations that are highly drug-loaded. This is attributed to the fact that the interfacial area created by a rise in lipid content necessitates a corresponding rise in surfactant coverage to provide successful stabilization.

Contour plots from factorial models produced a visual illustration of the relationship between independent variables and responses (**Fig. 3**). From these plots, optimum formulation spaces were observed that were defined by optimal combination of particle size less than 100 nm, PDI less than 0.30, encapsulation efficiency more than 94%, and acceptable drug loading more than 12%. The polynomial model equation is as under:

$$Y_1 = 132.8 + 28.65X_1 - 43.72X_2 + 8.34X_1X_2 + 12.45X_1^2 + 15.23X_2^2$$

$$Y_2 = 0.322 + 0.060X_1 - 0.083X_2 - 0.020X_1X_2 + 0.017X_1^2 + 0.040X_2^2$$

$$Y_3 = 95.67 + 2.34X_1 + 1.87X_2 - 0.12X_1X_2 - 3.12X_1^2 - 2.45X_2^2$$

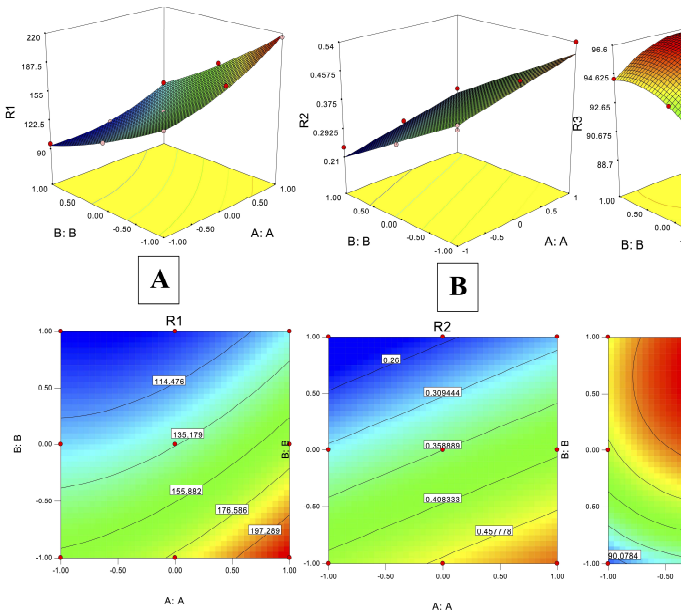

Fig. 3. Response surface contour plots illustrating the effects of drug-to-lipid ratio (X_1) and surfactant concentration (X_2) on (A) particle size, (B) polydispersity index, (C) encapsulation efficiency, and (D) overall desirability.

Checkpoint Analysis

To further validate the predictive capability of the developed quadratic models, checkpoint analysis was conducted using formulations not included in the original 3^2 factorial design. Selected checkpoint batches as shown in **Table 3** were prepared and their experimental responses were compared with the corresponding predicted values generated by the polynomial equations. The percent prediction error for particle size, PDI, and encapsulation efficiency remained below 5% for all checkpoint formulations, thus establishing the robustness and reliability of the response surface models, and their external validity as well. This verification step further supports the suitability of the models for guiding formulation optimization.

Lastly, desirability function optimization

(and objectives of particle size minimization, PDI minimization and encapsulation efficiency maximization) the best formulation parameters were found as: drug-to-lipid ratio of 1:15.2 and surfactant concentration of 3.8% w/v. The predicted values of the particle size, PDI, and encapsulation efficiency were 102.3 nm, 0.28, and 95.8 respectively. The contour maps illustrate the interactive effects of each variable of the formulation and points to the design space where the best nanoparticle properties are obtained. Areas with smaller sizes, lower PDI, and better encapsulation efficiency are drawn to the highest desirability zone, which in favor of the selected optimized formulation.

Table 3 Checkpoint Analysis for Model Validation of RSM Predictive Performance

Checkpoint Batch	Response	Predicted Value	Experimental Value	% Prediction Error
CP1 (X_1 = -0.5, X_2 = 0)	Particle Size (nm)	149.3	151.1	1.20%
	PDI	0.34	0.33	2.94%
	Entrapment Efficiency (%)	92.1	90.2	2.06%
CP2 (X_1 = +0.5, X_2 = +0.5)	Particle Size (nm)	134.3	130.4	2.91%
	PDI	0.32	0.33	3.13%
	Entrapment Efficiency (%)	96.4	95.6	0.83%
X1 = Drug: Total lipid concentration X2 = % Surfactant				

Physicochemical Characterization of Optimized NLCs

The physicochemical properties are especially sought after in nano formulations made of nutraceuticals, with stability and uniformity having a direct effect on absorption, distribution, and long-term safety.

Transmission electron microscopy showed that the BONLCs had a spherical shape and smooth surface features (**Fig. 4**). The cellular uptake is beneficial due to the spherical architecture where the surface area to volume ratio is minimized, and endocytic internalization is easily reduced [58]. The lack of aggregation of particles or irregular shape was a confirmation of the efficiency of the surfactant system chosen in offering long-term colloidal stability.

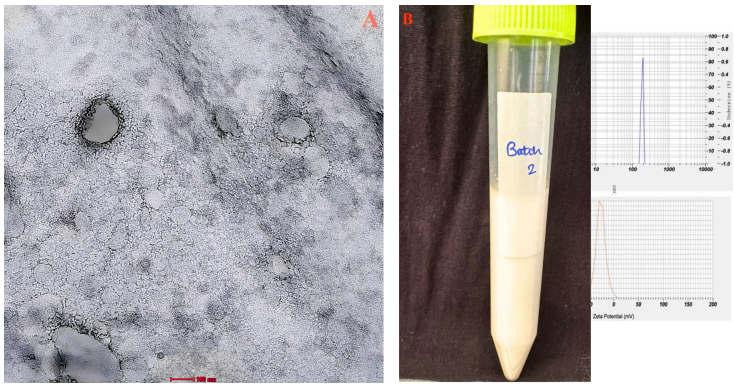

Fig. 4. (A) The microscopic image of optimized BONLCs as seen using TEM analysis and (B) the optimized BONLCs

Surface Charge and Particulate Size.

A dynamic light scattering analysis revealed that the BONLCs were optimized with a mean particle size of 100.5 ± 4.2 nm and polydispersity index of 0.26 ± 0.03, which indicates a narrow size distribution and high reproducibility of a batch to another as presented in **Fig. 5**. Comparatively, OANLCs exhibited a marginally higher particle size (174.3 ± 5.7 nm PDI 0.31 ± 0.04), which could be explained by variations in the lipid composition and crystallization behavior

between borage oil and oleic acid.

Zeta potential of the samples showed that BONLCs had a surface charge of -32.4 ± 2.1 mV. The anionic phospholipid constituents of the soy lecithin and carboxylic acid groups of the free fatty acids of the borage oil can be attributed to the negative surface charge. Zeta potential values greater than -30 mV or +30 mV are typically taken to be evidence of a high level of colloidal stability, because undergoes the DLVO (Derjaguin-Landau-Verwey-Overbeek) theory mechanisms of repulsion prevent aggregation of particles in strong electrostatic repulsion [59]. The size of the submicron particle and good surface charge properties indicates that these NLC formulations can be used to deliver the systemically and could have increased cellular uptake via size-sensitive endocytic routes.

Fig. 5. The particle size distribution of (a) BONLCs (b) OANLCs and the zeta potential of (c) BONLCs and (d) OANLCs respectively

Drug loading and Encapsulation Efficiency.

Spectrophotometric analysis of the samples showed that the encapsulation efficiency of BONLCs (98.53 ± 1.21) was higher than that of OANLCs (92.12 ± 2.34), indicating that Borage oil-based formulation had a higher drug retention capacity. Mechanical means of this improved encapsulation can be explained by the existence of favorable molecular interactions between resveratrol and the polyunsaturated fatty acid constituents of the borage oil, especially the GLA, which can be induced to form hydrogen bonding networks with the hydroxyl groups of resveratrol [60,61].

In Vitro Kinetics of Drug Release.

The release kinetics were mathematically modeled, which showed that both formulations were dominated by Higuchi diffusion-controlled release (R^2 > 0.95), and supplemented by Fickian diffusion. The Korsmeyer-Peppas model produced release exponent (n) of 0.45-0.60, which was an indication of anomalous (non-Fickian) transport with a combination of drug diffusion and relaxation/erosion of the matrix [62-65].

The biphasic release profile (**Fig. 6**) exhibited by BONLCs is clinically beneficial as the first burst release yields immediate attainment of therapeutic drug levels, and the second stage of release sustains effective levels during long periods. This mode of release is beneficial to nutraceutical-based interventions that are to be used in the management of chronic diseases especially in cancer treatment where acute cytotoxic effects and long term exposure to the drug is desirable to ensure that tumor cell growth and drug resistance are inhibited [66-69]. Conversely, OANLCs portrayed a more gradual, sustained discharging, possibly restricting prompt treatment.

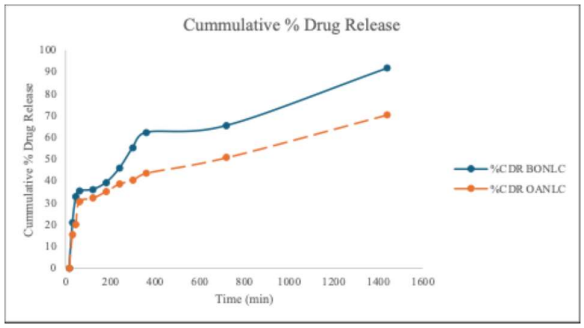

Fig. 6. Plot of comparative cumulative % drug release from BONLC and OANLC.

Cytotoxicity and Antiproliferative Analysis.

The antiproliferative effect of free resveratrol, BONLCs, and OANLCs on A549 NSCLC cells was analyzed in comprehensive cytotoxicity studies. MTT assays indicated that all the tested formulations had concentration-dependent cytotoxicity, and NLC-based delivery systems had a significantly greater potency

than free drug (**Fig. 7**).

Free resveratrol had an IC_{50} of 38.91 ± 3.82 5M, which is comparable to the existing reports of the same substance in A549 cells [70,71]. Lipid-based nanocarrier systems significantly enhanced cytotoxic potency compared to free drug [56]. OANLCs demonstrated significantly improved cytotoxic efficacy with an IC_{50} of 20.67 ± 1.93 μM, representing a 1.8-fold enhancement in potency. Most notably, BONLCs exhibited the most pronounced antiproliferative effects, achieving an IC_{50} value of 10.22 ± 1.34 μM—corresponding to a 3.8 -fold improvement relative to free resveratrol and a 1.45-fold enhancement compared to OANLCs [56].

The GLA-rich borage oil component exerts independent anticancer effects through multiple mechanisms including modulation of prostaglandin synthesis, induction of oxidative stress in cancer cells, and perturbation of cellular membrane integrity [32,72-74]. The combination of resveratrol and GLA produces synergistic cytotoxicity, as confirmed by Q-value analysis [33, 75,76]. Collectively, these results demonstrate that rational integration of nutraceutical bioactive within nanostructured lipid carriers can significantly amplify anticancer efficacy through synergistic and multi-mechanistic pathways.

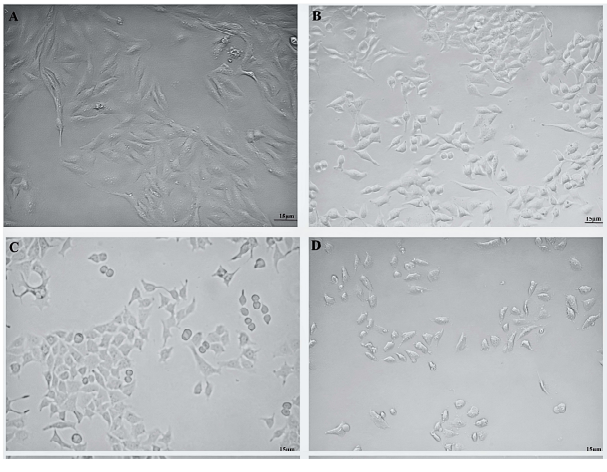

Fig. 7. Image of MTT Assay after 24 hrs. A) control B) treated with free RSV C) treated with OANLCs d) Treated with BONLCs

Conclusion

The present work demonstrates a rational nutraceutical-enabled nanotechnological approach to address key formulation and pharmacokinetic limitations associated with resveratrol in non-small cell lung cancer. NLCs were designed by strategic choice of a GLA-rich nutraceutical oil (borage oil) as bioactive lipid, that is, to combine both excipient functionality and therapeutic effects enabling high levels of solubilization, encapsulation efficacy, and antiproliferative efficacy. The NLCs prepared using borage oil showed good physicochemical characteristics such as nanoscale size with a narrow size distribution, high colloidal stability, and drug encapsulation. These carriers had a substantial functional enhancement of anticancer activity over free resveratrol and traditional oleic acid-based preparations with an increase of IC 50 in 3.8-fold. This was boosted by the synergistic effect between the GLA-rich bioactive excipient and resveratrol as evidenced by the in vitro synergistic effect. Also, the biphasic drug release profile promotes rapid early pharmacological action as well as long-term exposure to drugs. Overall, the results highlight the significance of rational excipient choice in the context of changing lipid nanocarriers into active delivery vehicles into bioactive and synergistic nanotherapeutic systems. This article emphasizes the possibility of combining nutraceutical bioactives and nanotechnology as a complementary one in treating chronic diseases. Additional research in the areas of in vivo performance, pulmonary bioavailability, and aerosolization behavior would be justified to proceed this platform to translational lung cancer nanomedicine.

References

1. Schabath MB, Cote ML. Cancer progress and priorities: Lung cancer. Cancer Epidemiol Biomarkers Prev. 2019;28(10):1563-1579.
2. Siegel RL, Giaquinto AN, Jemal A. Cancer statistics, 2024. CA Cancer J Clin. 2024;74(1):12-49.
3. Sung H, Ferlay J, Siegel RL, et al. Global cancer statistics 2020: GLOBOCAN estimates. CA Cancer J Clin. 2021;71(3):209-249.
4. Herbst RS, Morgensztern D, Boshoff C. The biology and management of non-small cell lung cancer. Nature. 2018;553:446-454.
5. Latimer KM, Mott TF. Lung cancer: Diagnosis, treatment principles, and screening. Am Fam Physician. 2015;91(4):250-256.
6. Wang X, Zhang H, Chen X. Drug resistance and combating drug resistance in cancer. Cancer Drug Resist. 2019;2:141-160.
7. Shi J, Kantoff PW, Wooster R, Farokhzad OC. Cancer nanomedicine: Progress, challenges and opportunities. Nat Rev Cancer. 2017;17(1):20-37.
8. Rosenblum D, Joshi N, Tao W, Karp JM, Peer D. Progress and challenges towards targeted delivery of cancer therapeutics. Nat Commun. 2018;9:1410.
9. Torchilin VP. Recent advances with liposomes as pharmaceutical carriers. Nat Rev Drug Discov. 2005;4(2):145-160.
10. García-Pinel B, et al. Lipid-based nanoparticles: Application and recent advances in cancer treatment. Nanomaterials (Basel). 2019;9:638.
11. Mitchell MJ, Billingsley MM, Haley RM, et al. Engineering precision nanoparticles for drug delivery. Nat Rev Drug Discov. 2021;20(2):101-124.
12. Müller RH, Mäder K, Gohla S. Solid lipid nanoparticles for controlled drug delivery. Eur J Pharm Biopharm. 2000;50(1):161-177.
13. Müller RH, Radtke M, Wissing SA. Solid lipid nanoparticles and nanostructured lipid carriers. Adv Drug Deliv Rev. 2002;54(suppl 1):S131-S155.
14. Beloqui A, Solinís MA, Rodríguez-Gascón A, Almeida AJ, Préat V. Nanostructured lipid carriers: Promising drug delivery systems. Nanomedicine. 2016;12(1):143-161.
15. Haider M, Abdin SM, Kamal L, Orive G. Nanostructured lipid carriers for delivery of chemotherapeutics. Pharmaceutics. 2020;12(3):288.
16. Athar M, Back JH, Tang X, et al. Resveratrol: Preclinical studies for cancer prevention. Toxicol Appl Pharmacol. 2007;224(3):274-283.
17. Singh CK, Ndiaye MA, Ahmad N. Resveratrol and cancer: Challenges for clinical translation. Biochim Biophys Acta Rev Cancer. 2015;1852(6):1178-1185.
18. Carter LG, D'Orazio JA, Pearson KJ. Resveratrol and cancer: In vivo evidence. Endocr Relat Cancer. 2014;21(3):R209-R225.
19. Feng Y, Zhou J, Jiang Y. Resveratrol in lung cancer: A systematic review. J BUON. 2016;21(4):950-953.
20. Yousef M, Vlachogiannis IA, Tsiani E. Effects of resveratrol against lung cancer. Nutrients. 2017;9(11):1231.
21. Mukherjee S, Dudley JI, Das DK. Dose-dependency of resveratrol in health benefits. Dose Response. 2010;8(4):478-500.
22. Salehi B, et al. Resveratrol: A

double-edged sword. Biomedicines. 2018;6(3):91.
23. Walle T. Bioavailability of resveratrol. Ann N Y Acad Sci. 2011;1215:9-15.
24. Smoliga JM, Baur JA, Hausenblas HA. Resveratrol and health: Clinical trials. Mol Nutr Food Res. 2011;55(8):1129-1141.
25. Sharan S, Nagar S. Pulmonary metabolism of resveratrol. Drug Metab Dispos. 2013;41(10):1806-1814.
26. Madni A, et al. Liposomal drug delivery: Clinical applications. J Pharm Pharm Sci. 2017;20:401-426.
27. Weber S, Zimmer A, Pardeike J. SLN and NLCs for pulmonary application. Eur J Pharm Biopharm. 2014;86(1):7-22.
28. Costabile G, et al. Inhalable lipid and polymer nanocarriers. Pharmaceutics. 2024;16(3):347.
29. Aditya NP, et al. Lipid nanocarriers for quercetin delivery. LWT Food Sci Technol. 2014;59(1):115-121.
30. Zhang Y, et al. Combination therapy enhances cytotoxicity. Cancer Lett. 2011;304(1):21-32.
31. Feng X, et al. Unification of medicines and excipients. J Drug Deliv Sci Technol. 2023;82:104352.
32. Begin ME, Das UN, Ells G. Selective killing by polyunsaturated fatty acids. Prostaglandins Leukot Med. 1985;19(2):177-186.
33. Das UN. Gamma-linolenic acid as anticancer agent. Nutrition. 1990;6(6):429-434.
34. Jóźwiak P, et al. GLA pathway genes in colorectal cancer. Biomolecules. 2020;10(1):130.
35. Fan YY, Chapkin RS. Dietary gamma-linolenic acid. J Nutr. 1998;128(9):1411-1414.
36. Mehnert W, Mäder K. Solid lipid nanoparticles. Adv Drug Deliv Rev. 2001;47(2-3):165-196.
37. Pardeike J, Hommoss A, Müller RH. Lipid nanoparticles in dermal products. Int J Pharm. 2009;366(1-2):170-184.
38. Gunstone FD. Gamma-linolenic acid properties. Prog Lipid Res. 1992;31(2):145-161.
39. Crozier GL, et al. Blackcurrant seed oil fatty acids. Lipids. 1989;24(5):460-466.
40. Battaglia L, Gallarate M. Lipid nanoparticles: State of the art. Expert Opin Drug Deliv. 2012;9(5):497-508.
41. Jin ZJ. About the evaluation of drug combination. Acta Pharmacol Sin. 2004;25(2):146-147.
42. Mosmann T. Rapid colorimetric assay for cell growth. J Immunol Methods. 1983;65(1-2):55-63.
43. Joshi MD, Müller RH. Lipid nanoparticles for parenteral delivery. Eur J Pharm Biopharm. 2009;71(2):161-172.
44. Paliwal R, et al. Nanomedicine scale-up technologies. AAPS PharmSciTech. 2014;15:1527-1534.
45. Ganesan P, Narayanasamy D. Lipid nanoparticles for oral delivery. Sustain Chem Pharm. 2017;6:37-56.
46. Ohkuma S, Poole B. Intralysosomal pH measurement. Proc Natl Acad Sci U S A. 1978;75(7):3327-3331.
47. Oh N, Park JH. Endocytosis of nanoparticles. Int J Nanomedicine. 2014;9:51-63.
48. Nyberg K, et al. Phagolysosomal pH in macrophages. Environ Health Perspect. 1992;97:149-152.
49. Zhang T, et al. NLC for oral delivery of etoposide. Eur J Pharm Sci. 2011;43(3):174-179.
50. Costa P, Sousa Lobo JM. Modeling dissolution profiles. Eur J Pharm Sci. 2001;13(2):123-133.

51. Peppas NA, Sahlin JJ. A simple equation for solute release. Int J Pharm. 1989;57(2):169-172.
52. Korsmeyer RW, et al. Solute release mechanisms. Int J Pharm. 1983;15:25-35.
53. Lasic DD. Liposomes: From Physics to Applications. Elsevier; 1993.
54. Patil YP, Jadhav S. Novel methods for liposome preparation. Chem Phys Lipids. 2014;177:8-18.
55. Qu D, et al. Microemulsion improves lung cancer therapy. Drug Deliv. 2017;24(1):1179-1190.
56. Wang Y, et al. Co-delivery by NLCs for lung cancer. Drug Deliv. 2016;23(4):1398-1403.
57. Hung SS, et al. Resveratrol combination therapy. Oncotarget. 2018;9(68):32943-32957.
58. Shi F, et al. Solid lipid nanoparticles with essential oils. Int J Nanomedicine. 2012;7:2033-2043.
59. Doktorovová S, et al. Preclinical safety of SLN and NLCs. Eur J Pharm Biopharm. 2016;108:235-252.
60. Yingchoncharoen P, et al. Lipid-based drug delivery systems. Pharmacol Rev. 2016;68(3):701-787.
61. Delmas D, et al. Transport and stability of resveratrol. Ann N Y Acad Sci. 2011;1215:48-59.
62. Higuchi T. Mechanism of sustained-action medication. J Pharm Sci. 1963;52(12):1145-1149.
63. Ritger PL, Peppas NA. Solute release equations. J Control Release. 1987;5(1):23-36.
64. Siepmann J, Peppas NA. Modeling of drug release from HPMC systems. Adv Drug Deliv Rev. 2001;48(2-3):139-157.
65. Siepmann J, Siepmann F. Mathematical modeling of drug delivery. Int J Pharm. 2008;364(2):328-343.
66. Uhrich KE, et al. Polymeric systems for drug release. Chem Rev. 1999;99(11):3181-3198.
67. Danhier F, Feron O, Préat V. Tumor targeting of nanocarriers. J Control Release. 2010;148(2):135-146.
68. Waheed S, Li Z, Zhang F, Chiarini A, Armato U, Wu J. Engineering nano-drug biointerface to overcome biological barriers toward precision drug delivery. J Nanobiotechnol. 2022;20(1):395. doi:10.1186/s12951-022-01605-4.
69. Gottesman MM. Mechanisms of drug resistance. Annu Rev Med. 2002;53:615-627.
70. Fan Y, et al. Resveratrol induces apoptosis in A549 cells. Int J Oncol. 2020;57(4):925-938.
71. Najafiyan B, et al. Resveratrol in lung cancer therapy. Biomed Pharmacother. 2024;172:116207.
72. Serini S, et al. PUFA-induced apoptosis. Apoptosis. 2009;14(2):135-152.
73. Stillwell W, Wassall SR. DHA and membrane properties. Chem Phys Lipids. 2003;126(1):1-27.
74. Kaviani E, et al. Omega-6 fatty acids and cancer. Mol Nutr Food Res. 2025;69(12):e70092.
75. Chou TC. Drug combination synergy quantification. Cancer Res. 2010;70(2):440-446.
76. Zhao L, Au JL, Wientjes MG. Drug–drug interaction methods. Front Biosci. 2010;2:241-249

Author Contributions

S. K. K. conceptualized the study design and curated data, conducted investigation and wrote the draft manuscript. A.N.M. conceptualized, corrected, and revised the draft manuscript. H.V.P supervised the project and provided essential resources.

Ethics approval and consent to participate
Not applicable.

Human and animal rights
Not applicable.

Consent for publication
Not applicable.

Availability of data and materials
The data and supportive information are available within the article.

Funding
None.

Conflict of interest
The authors declare no conflict of interest, financial or otherwise

Abbreviations
NSCLC – Non-Small Cell Lung Cancer
COPD – Chronic Obstructive Pulmonary Disease
GLA – Gamma-Linolenic Acid
RSV – Resveratrol
NLCs – Nanostructured Lipid Carriers
BONLCs – Borage Oil-based Nanostructured Lipid Carriers
OANLCs – Oleic Acid-based Nanostructured Lipid Carriers
SLN – Solid Lipid Nanoparticles
OA – Oleic Acid
PDI – Polydispersity Index
EE (%) – Encapsulation Efficiency
DLS – Dynamic Light Scattering
TEM – Transmission Electron Microscopy
HR-TEM – High-Resolution Transmission Electron Microscopy
MTT – 3-(4,5-dimethylthiazol-2-yl)-2,5-diphenyltetrazolium bromide
DMSO – Dimethyl Sulfoxide
FBS – Fetal Bovine Serum
CO_2 – Carbon Dioxide
IC_{50} – Half Maximal Inhibitory Concentration
OFAT – One Factor At a Time
RSM – Response Surface Methodology
ANOVA – Analysis of Variance
R^2 – Coefficient of Determination
X_1 – Independent Variable 1 (Drug-to-lipid ratio)
X_2 – Independent Variable 2 (Surfactant concentration)
Y_1 – Particle Size
Y_2 – Polydispersity Index
Y_3 – Encapsulation Efficiency
Q-value – Combination Index (Synergism Indicator)
ALF – Artificial Lysosomal Fluid
Da – Dalton
HLB – Hydrophilic-Lipophilic Balance
RHLB – Required Hydrophilic-Lipophilic Balance

Acknowledgements
The authors gratefully acknowledge the Department of Applied and Interdisciplinary Sciences, Sardar Patel University, Vallabh Vidyanagar, Anand, Gujarat for providing the facilities of cell culture laboratory and supporting with the animal cell line studies. The authors are also obliged to Sophisticated Instrumentation Centre for Applied Research and Testing – SICART, Charutar Vidya Mandal for the transmission electron microscopy facility provided for conducting the research.